

DOI: 10.5281/zenodo.4916515

NON-DESTRUCTIVE STUDY OF GOLD ARTEFACTS WITH PROMPT ATOMIC AND NUCLEAR METHODS

Guy Demortier

LARN - University of Namur (Belgium), 61 rue de Bruxelles - B 5000 Namur (Belgium)
(*guy.demortier@unamur.be*)

Received: 25/05/2021

Accepted: 20/06/2021

ABSTRACT

Accelerator based analytical tools have been used for quantitative analysis of gold artefacts. Proton, deuteron and alpha particle energies are limited to avoid any residual activity after the irradiation of the precious items. Surface depletion gilding and soldering procedures used in ancient goldsmith's technologies are firstly identified and then reproduced in laboratory. A selection of 9 representative artefacts belonging to pre-Hispanic American, Byzantine and Roman Cultures are selected to illustrate human skill in ancient times. The meaning of santerna or chrysocola reported in the Plini's Natural History is discussed.

KEYWORDS: gold jewellery, PIXE, RBS, NRA, non-destructive microanalysis, depletion gilding, pre-Hispanic gold, Achaemenid, greenockite, Monte Alban, Selemieh

1. INTRODUCTION

The ambition of archaeology is the rediscovery of many aspects of human activity. Artefacts are a part of the archaeological testimony of ancient societies. Archaeologists and museum curators call on scientists for the analysis of their artefacts. Since 1979 nuclear physicists of LARN (Laboratoire d'Analyses par Réactions Nucléaires) are involved in this field for non-destructive analyses of gold objects. The experimental equipment of LARN is based on a Tandem electrostatic 2 MV accelerator for the production of particle beams (protons, deuterons, α particles...). The incident particle energy is too low to induce residual activity after irradiation of materials.

Archaeologists, historians, museum curators were convinced of the absence of damage by our experience in the in-vivo study of fluorine in tooth enamel (Demortier 2021) as illustrated in Fig. 1. LARN equipment was also used by our colleagues of France to support the creation, in 1987, of AGLAE: Accélérateur Grand Louvre pour l'Analyse Élémentaire (Amsel et al. 1986).

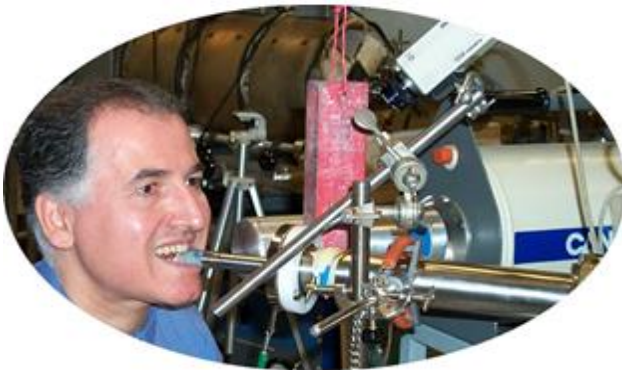


Figure 1: Non-vacuum PIXE is safe

Particle-induced-X-ray (or γ -ray)-emission (PIXE or PIGE) associated with Rutherford-backscattering-spectroscopy (RBS) are powerful tools for the study of thin layers below the surface (about 10-20 μm). They can be ideally applied for the analysis of gold based materials which are generally preserved from corrosion.

More than 200 ancient gold artefacts were studied at LARN: they belong to several museums (Berlin,

Cluny, Louvre, Madrid, Mexico, Oaxaca, Poitiers, Rhode Island, Seville, Tongres, Tournai, Troyes) and sometimes to private owners. Details may be found in selected publications (Demortier and Hackens 1982; Demortier 1983; Demortier 1984; De Cuyper et al. 1987; Ruvalcaba and Demortier 1996; Ontalba-Salamanca et al. 1998; Montero et al. 2001). Other artefacts from Italy, Slovenia and Tajikistan were studied in collaborations with scientists of Ljubljana, Lecce, Orleans and Paris. (Smit et al. 2000; Demortier et al. 2008; Guerra et al. 2009). Gilded techniques and an archaeometry overview as relevant overall analyses is reported recently (Liritzis et al., 2020).

The present review paper will concentrate on the use of PIXE and PIGE to identify various methods of gold brazing and/or gold soldering on spectacular artefacts belonging to European collections and the depletion gilding performed on pre-Hispanic Mexican jewellery. Reproduction in LARN of ancient goldsmith's technologies and careful interpretation of ancient recipes will be added to support the analytical results.

2. ACCELERATOR-BASED EXPERIMENTAL TOOLS

2.1 PIXE (*Particle Induced X-ray Emission*)

The emission of X-rays induced by protons in materials is similar to that induced by electrons. Electron or proton beams disturb the electronic structure of target atoms which rapidly return to a lower energy state partially by characteristic X-ray emission. The name PIXE was proposed by Sven Johansson in 1970 (T.B. Johansson et al. 1970). The main difference in the respective trajectories is illustrated in Fig. 2 for two usual configurations: 20 KeV electrons versus 2.5 MeV protons on a gold target. Incident protons on Au (a system of 79 electrons surrounding one single nucleus) follow a straight line at least for the main part of their trajectory. Shell electrons of irradiated material cannot deflect protons due to their big mass difference. The proton deviation could only occur at the end of the trajectory when they are sufficiently slow to spend some interaction time in the vicinity of the atomic nucleus.

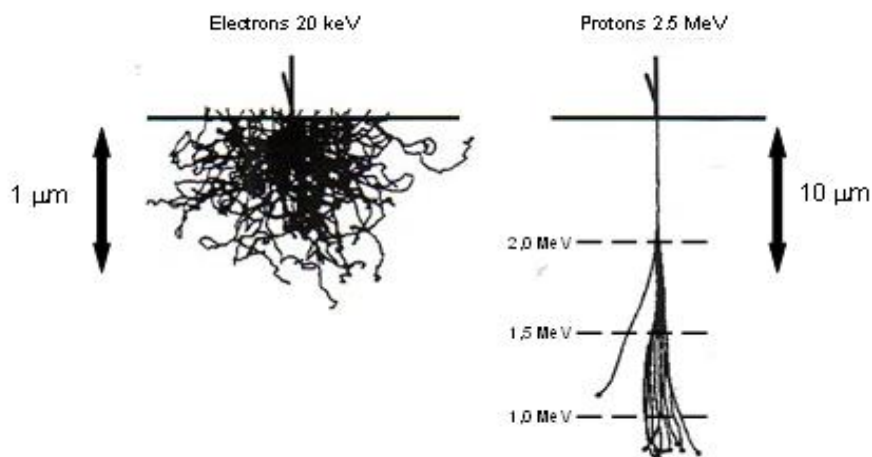


Figure 2: Range of electrons and protons in gold

2.2 Non-vacuum PIXE

One takes advantage of that proton trajectory to extract the beam from the evacuated tube of the accel-

erator (Fig.3) in order to irradiate the artefact at atmospheric pressure. Narrow regions on large artefacts may be studied with proton beams of less than 1 mm in diameter as shown in Fig. 4.

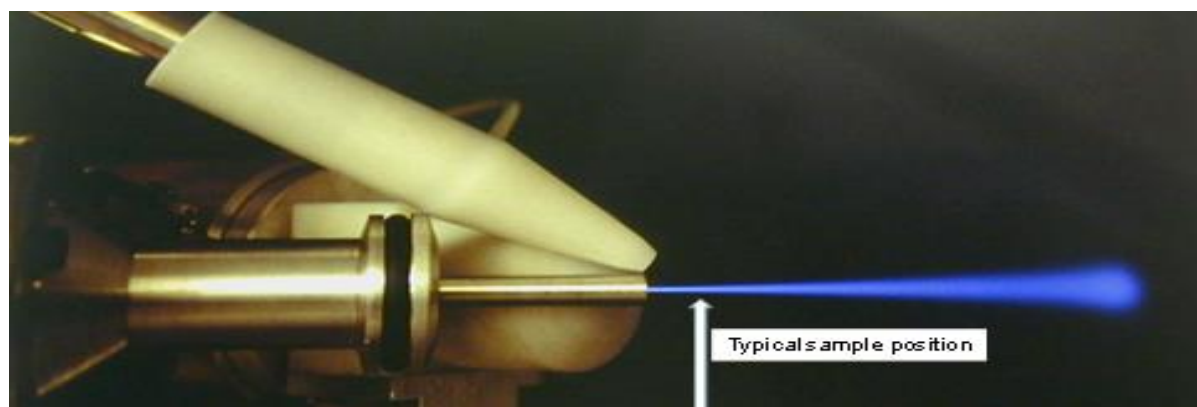


Figure 3: 2.5 MeV protons in air



Figure 4: Non-vacuum PIXE for analysis of large artefacts

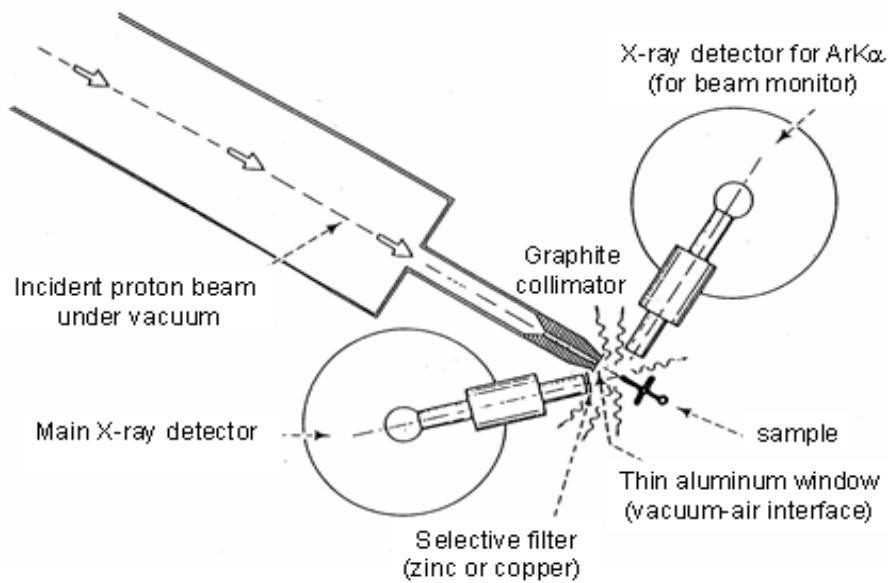


Figure 5: Non-vacuum PIXE set up

The experimental arrangement is schematically shown in Fig.5: the incident proton beam is extracted from the accelerator through a tin Al foil (7 μm thick) and hit the sample after crossing 1 cm in air. X-rays produced in argon present in the air between the exit foil and the artefact are collected in the lateral X-ray Si(Li) detector in order to monitor successive measurements. X-rays induced in the irradiated artefact are collected in the main detector. As the intensity of gold L X-ray lines is extremely important, a filter of zinc (20 μm thick) is inserted in front of the main detector in order to selectively reduce the intensity of gold X-ray L- lines. The transmission is drastically reduced down to 2.2% and 8.65% for $L\alpha$ and $L\beta$ lines of Au respectively but only to 42.8% and 66.3% for the $K\alpha$ line of Cu and Ag. For most applications on gold artefacts a counting rate of about 2 000 photons per second is acceptable to limit the intensity of pile-up peaks of K lines of Cu with L lines of Au (see the 15 arrows from 16.1 keV to 24.3 keV) at a level behind

1% relative to L X-ray lines of Au. The contribution of these pile-up peaks is taken into account for the calculation of X-ray intensities.

Escape peaks (1.74 and 1.84 keV below the main peak for Si(Li) detectors) are not clearly observable except for $K\alpha\text{Cu}$ (Fig.6).

The computation of elemental concentrations of Cu, Au and Ag is based on the X-ray cross section data (Cohen 1999) briefly summarized in Fig.7 for the elements of interest (including the reduction of intensity by the Zn absorber) but takes also into account the complicated self absorption of various X-ray signals in the ternary Cu-Au-Ag alloy.

Details of absorption are given in Fig. 8. Special attention has been taken on the region between 21 and 25 keV corresponding to K lines of Ag and Cd. The zinc filter is so thick that no X-ray signal below 5 keV can be detected (in particular X-ray lines of Al produced in the exit foil). Elements of atomic number below 24 (Cr) cannot be identified.

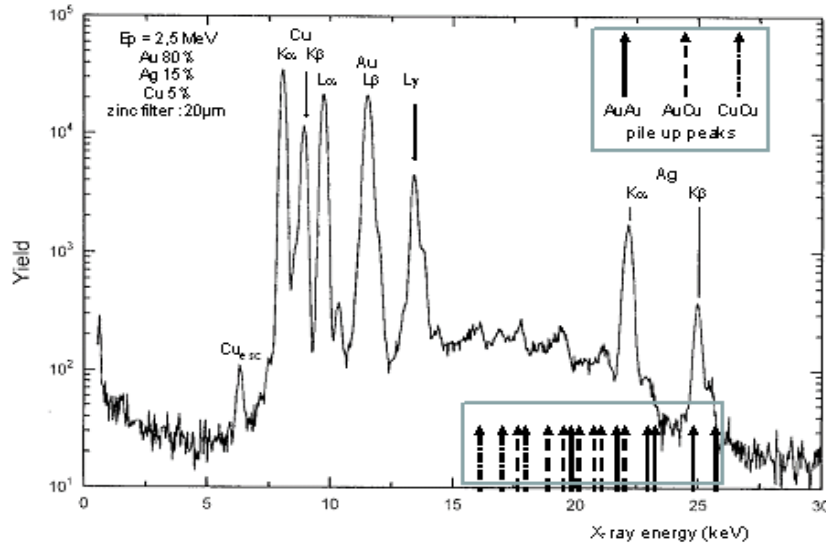


Figure 6: PIXE spectrum of Au-Ag-Cu alloy and position of sum peaks

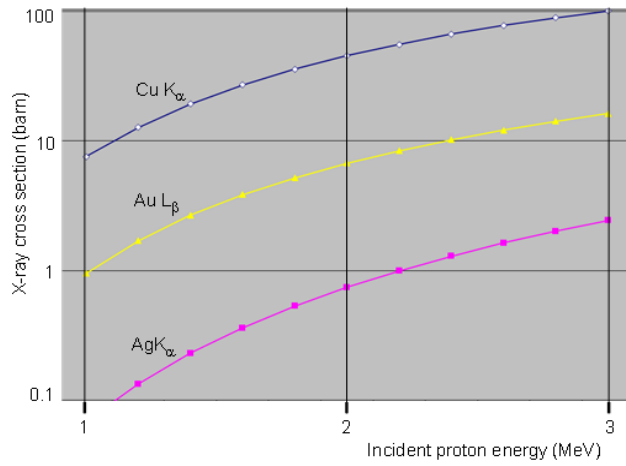


Figure 7: X-ray intensities for CuK α , AuL β and AgK α lines with 20 μ m Zn absorber

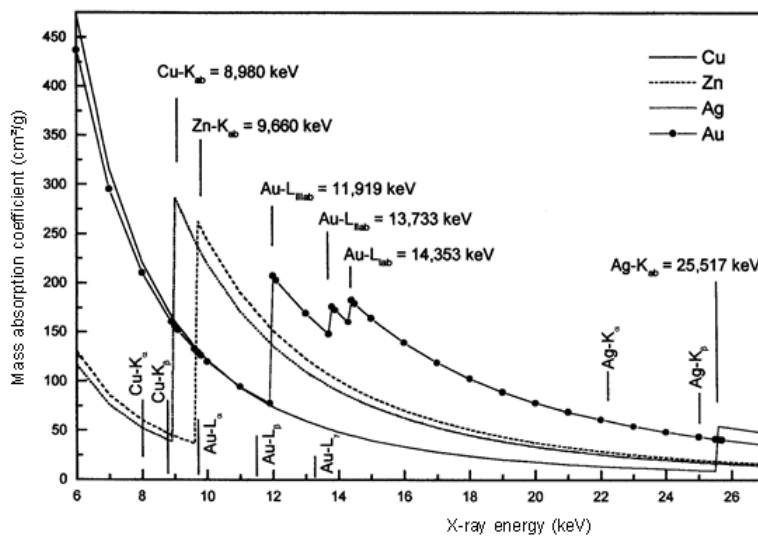


Figure 8: X-ray absorption coefficient in Au, Ag, Cu and Zn

2.3 In vacuum PIXE and Rutherford backscattering spectroscopy (RBS)

PIXE with external particle beams (mainly protons) became widely popular since the demonstration in 1971 of its capability to non-destructive analysis any kind of material including liquids and fragile samples (Deconninck 1971, Deconninck 1978) as clearly illustrated in figure 1 for in-vivo study of tooth enamel. At that time the name "PIXE" was not yet widely used and Deconninck refers to (p,X) reactions. PIXE is also used in combination with Rutherford backscattering spectroscopy (RBS) to verify if the surface composition of the object is different from that in the bulk. As far as gold rich artefacts are concerned the combination of PIXE with RBS brings new information on potential treatments which could have been applied to give a golden appearance to artefacts made with alloys of lower gold content. The irradiation takes place in a vacuum chamber. Backscattered particles are detected with a surface barrier detector and the emitted

X-rays and γ -rays are collected through a thin window in appropriate detectors as illustrated in Fig. 9. Typical RBS spectra collected in the backward direction (close to 180° relative to the incident proton beam) are given in Fig.10 for pure gold, silver and copper. Differences appear in two ways: the backscattered proton energy $E_s = KE_0$ with $K = (M-1/M+1)^2$ which gives 0.997 for gold, 0.934 for Ag and 0.940 for Cu. The difference is so small that information on gold contribution is only completely interference free in the first $0.15 \mu\text{m}$ below the surface. Fortunately, the cross section for elastic proton scattering varies with the Z^2 of the scattered nucleus and is then 2.8 and 7.4 times greater for Au than for Ag and Cu respectively as seen on the ordinates in figure10. For a basic alloy Au (80%), Ag (10%) and Cu (10%) the intensity of the scattered protons on gold is 22.4 and 59.4 times greater than for silver and copper respectively.

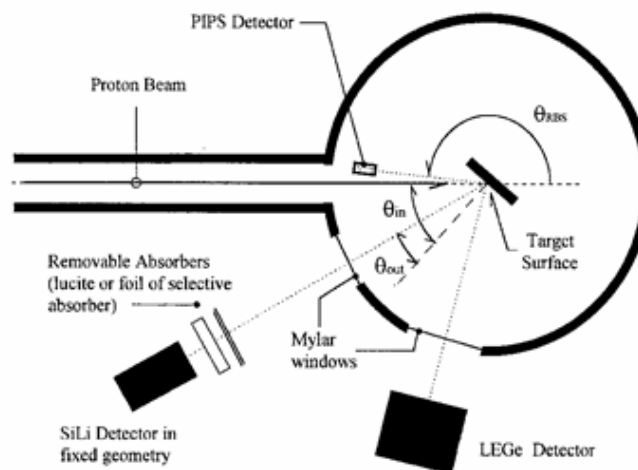


Figure 9: Microprobe arrangement for PIXE- RBS- NRA

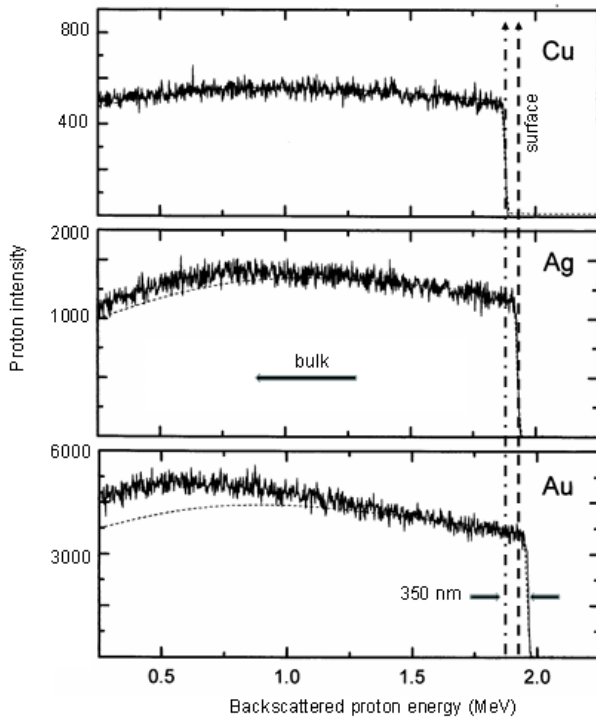


Figure 10: 2 MeV (protons) RBS spectra on pure elements

Simultaneous RBS and PIXE at various proton energies: a technology called differential PIXE (Van Oystaeyen and Demortier 1975; Demortier and Ruvalcaba 1996; Ruvalcaba 1997) was successfully used in the study of pre-Hispanic items made with tumbaga (the name for a non-specific alloy of gold and copper given by Spanish Conquistadores to metals composed of these elements). Surface enrichment (or depletion) of gold may be rapidly identified when

two PIXE measurements are performed with incident proton beams normal to the sample surface and repeated at the same place at grazing incidence on the artefact and on a certified homogeneous alloy also irradiated in normal and grazing incidences (Ruvalcaba 1997).

Nuclear reactions induced by α -particles and or ^3He were used as additional tools for a study of corrosion in pre-Hispanic jewellery (Ruvalcaba et al. 1997, Ruvalcaba 1997).

2.4 XRF induced by PIXE

Gold alloys for modern jewellery sometimes contain a few % of Zn and Cd. As characteristic X-ray lines of Zn (8.6 and 9.6 keV) strongly interfere with L1 and L α lines of Au (8.5 and 9.4 keV), PIXE cannot be used for Zn analysis. To get around this difficulty a special arrangement was installed (Fig. 11). The goal is to induce the ionization of the K shell electrons of Zn (9.96 keV) but not the L3 shell of Au (11.92 keV). The solution is to irradiate a Ge target to produce GeK α and GeK β X-rays (9.9 keV and 10.8 KeV) in order to selectively ionize the K shell of Zn in a very tight geometry (Fig. 12). X-rays produced by proton irradiation of ultra pure Ge can reach the artefact but also various collimators. These collimators are made with Lucite ($\text{C}_5\text{H}_8\text{O}_2$)_n or pure silicon in order that any X-ray signal entering the Si(Li) detector could have been produced in the artefact only. Traces of Zn down to 150 ppm in a gold rich matrix have been detected by this technique (Demortier 1987a). For additional gadget tools see (Demortier and Morciaux 1994).

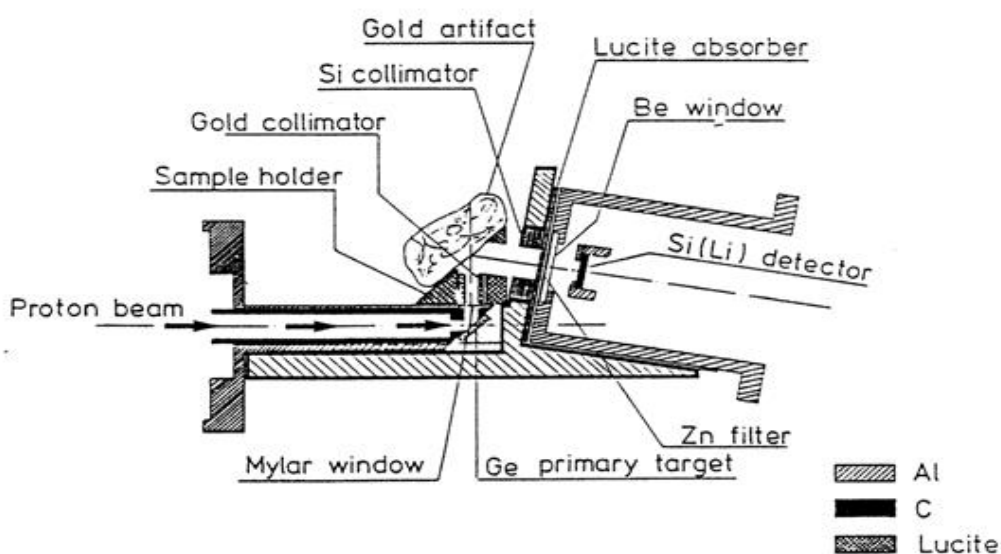


Figure 11: Special arrangement for XRF induced by PIXE (Ge primary target)

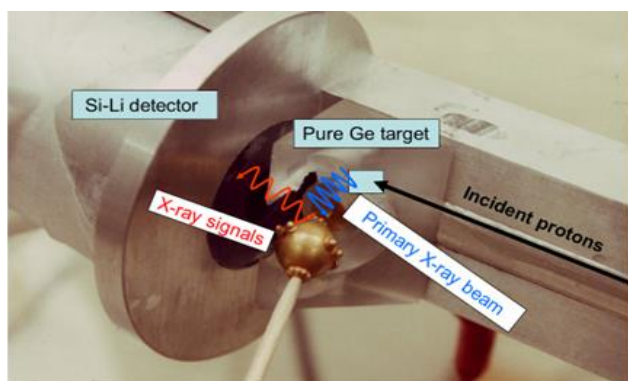


Figure 12: Study of a gold artefact by XRF induced by PIXE

2.5 PIXE microprobe

The size of proton beam used in non vacuum PIXE cannot be focussed on surfaces less than 500-700 μm in diameter due to the angular straggling in the air between the exit foil and the sample. Modern nuclear microprobes working in vacuum are now extensively used with a spatial resolution below 1 μm for beam intensities of 100 pA (Vavpetic et al., 2017). The artefact is then irradiated into a vacuum chamber but X-ray detectors take place outside the vacuum like for non-vacuum PIXE.

2.6 Nuclear methods of analysis of light elements

Light elements in gold artefacts cannot be analysed with PIXE due to the very high absorption of their low energy X-rays. As minerals have been directly used in ancient metallurgy (malachite, chalcocite, and other minerals containing Al or Si) to obtain specific alloys (in particular soldering alloys) traces of light elements like C, N, Al, Si, S could be locally present in the artefact. Deuteron induced nuclear reactions leading to proton emission offer an acceptable solution. The whole procedure is then operated in vacuum (Demortier and Gilson 1987). Exotic nuclear reactions induced by $^3\text{He}^+$ ions (namely $(^3\text{He},p)$ and $(^3\text{He},\alpha)$ reactions) are scarcely applied to clarify the structure of corroded surfaces of artefacts with low gold content (Ruvalcaba 1997).

2.7 Gamma-ray transmission for hollow artefacts

Large artefacts are generally made by lost wax technique and some internal cavity may be empty or filled with remains of the casting procedure (clay or other silicate material). Ancient torque bracelets are generally empty or shaped around some light structure to maintain its rigidity. Traditional methods of density measurement may give preliminary information on the presence of gold free regions. The arte-

fact is attached on a frame of Lucite and is moved vertically to finely scan its full thickness (Fig. 13). A collimated γ -ray beam (1 mm in diameter drilled in a set of lead shield 7 cm long) may be used for XRF and transmission analysis. ^{137}Cs for a single energy photon source ($E_\gamma = 662$ keV) or ^{226}Ra for a larger number of low energy γ -rays (186 KeV, 242 keV, 295 keV, 651 keV) depending on the size of the artefact have been successfully used (Demortier et al. 1999).

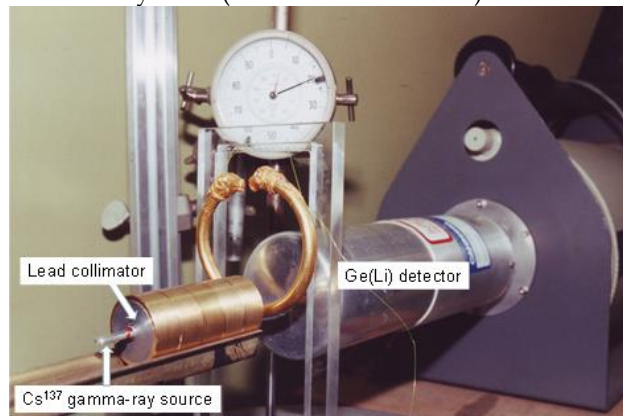


Figure 13: γ -ray transmission equipment for large artefacts

2.8 Reference materials

Analytical results on all gold artefacts refer to comparative concentrations of Cu, Ag, Au with certified commercial 18 carat gold alloys (Degussa and Lyon-Allemand) which were irradiated in the same experimental conditions. A careful control of the concentrations in each reference material was performed by comparison with pure metals by simultaneous PIXE and PIGE technologies. PIGE is similar to PIXE but concerns the detection of γ -rays. These γ -ray energies (in the region of MeV) are completely transmitted outside the irradiated material (Deconninck and Demortier 1975). Most of the PIXE measurements have been made using the certified sample J 750 -1 (Comptoir Lyon-Allemand Louyot): Au 750‰, Ag 60‰, Cu 90‰, Zn 60‰ and Cd 40‰.

3. ANCIENT GOLDEN ARTEFACTS FROM SOUTH AMERICA

Flat artefacts are certainly the easiest samples to be investigated. The analysed depth with protons of energy ranging between 2.5 MeV does not exceed 20 μm . Protons lose progressively their energy along their trajectory in straight line (see Fig. 2) by interaction with the shell electrons and the subsequent emission of characteristic X-rays. The X-ray intensity produced on the most abundant atoms (Cu, Ag and Au) rapidly decreases by a factor of 10 as proton energy is less than 1 MeV (see Fig.7). This analysed thickness of about 20 μm below the surface is the bulk composition for homogeneous samples like commercial 18

carat gold. One way to check the sample homogeneity is to compare the intensity of X-rays produced by each component (Cu, Ag, Au) of the flat artefact with the X-ray intensity produced by the homogeneous reference by repeated irradiations under various tilted positions: at normal incidence the analysed thickness is twice the one analysed by tilting by 60°. The inconvenience is that the irradiated surface is also twice greater when the analysed depth is twice lower. An alternative is to compare X-ray intensities of each component at various incident proton energies.

The solar disk (Fig. 14) from Tolima (Colombia - 200 - 1200 AD) seems have to be made with a very rich golden alloy. Nevertheless, its density is closer to that of copper than that of gold. It was studied in the non vacuum PIXE configuration of Fig. 5. The raw concentrations in Au, Ag and Cu at 3 impacts for 2.6 MeV protons compared with the uniform reference material indicate that the results are not compatible with the density measurement (raw concentration means true bulk concentration for a homogeneous alloy). The solar disk is certainly non homogeneous (Fig. 14-

b) and several measurements were then repeated at one single impact (centre n°1) at proton energies ranging from 0.6 to 2.6 MeV (Fig. 14-c). One observes a systematic decrease of the apparent gold content when the incident proton energy increases: in other words, the contribution of the bulk increases for increasing proton energies. Surface concentration of gold is therefore higher than in the bulk: a sign of applied surface treatment. Differential PIXE was combined with RBS in the configuration of figure 9 to clarify the situation. The depth distribution of Au, Ag and Cu of Fig. 14-d is in agreement with combined RBS and PIXE results at 8 proton energies. The full explanation is reported in (Demortier and Ruvalcaba 1996). Craftmen of Tolima have certainly operated a depletion gilding procedure on tumbaga to give an apparent pure golden aspect to the artefact made with a basic alloy (Au 68%, Cu 28% and Ag 6%). Depletion gilding has been extensively used in pre-Hispanic jewelry (Bray 1993) and the technique was reproduced at LARN by Jose Luis Ruvalcaba during his PhD thesis (Ruvalcaba 1997).

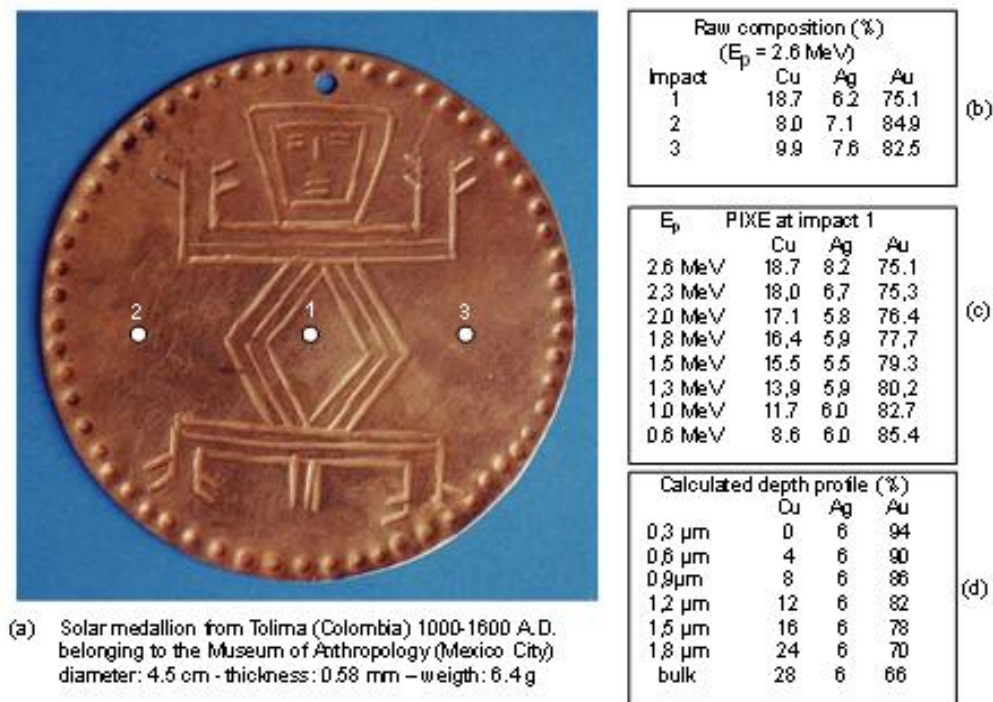


Figure 14: Depth profile measurement by non-vacuum PIXE at various proton energies

Depletion gilding is very simple. When heated up to 500°C the surface of a low-grade gold alloy (Au-Ag-Cu) shows a thin blackish surface indicating the production of metallic oxides (mostly copper oxides). After immersion in weak acid (a mixture of oxalic and citric acid) and heated below the boiling temperature, the alloy loses his blackish aspect: some copper is eliminated showing a frosted surface which is then

rubbed with a soft fabric. If the process is repeated several times one obtains a perfect golden aspect.

Non-vacuum PIXE analysis of the anthropomorphic pendant of Tairona culture (from 300 to 800 AD) (Fig. 15a) at 25 impacts on the front face has shown large variations of Cu and Au concentrations partially due to the roughness of the surface. It seems it was manufactured by the lost wax technique. The central body is partially empty but it was not possible

to estimate the density. The rear face is very flat and the ratio Cu / Au is nearly constant. The artefact was then introduced in the vacuum chamber to perform PIXE and RBS at 9 different proton energies from 0.8 to 2 MeV. RBS spectrum at 2.0 MeV clearly indicates that the surface Au content is significantly higher

than in the bulk (figure 15b). Computed PIXE and RBS data are summarized in Fig. 15c. Depletion gilding was applied so that copper was eliminated from the top surface layer: the original copper concentration (28% in the bulk) was gradually reduced down to nearly zero at surface.



(a) Anthropomorphic pendant
Tairona culture (Columbia) 600-1600 A.D.
6 cm x 4.6 cm x 1.5 cm (27.6 g)
National Museum of Anthropology Mexico

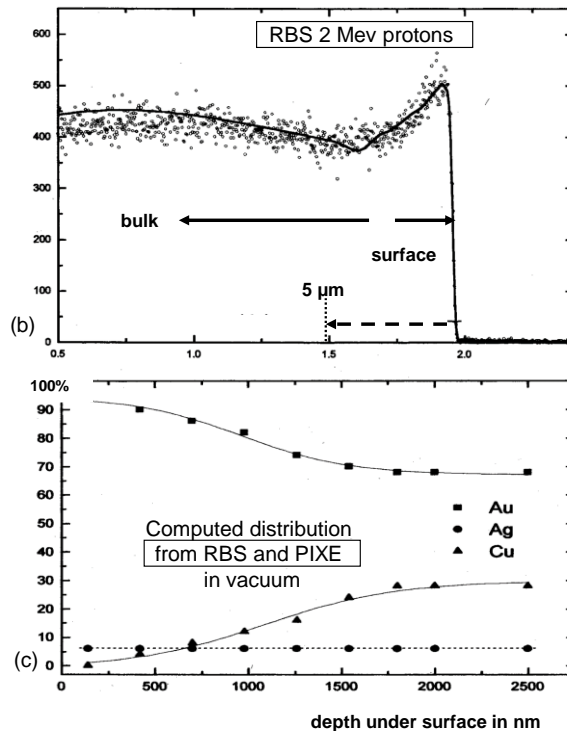


Figure 15: Depth profile measurement by combined RBS and PIXE

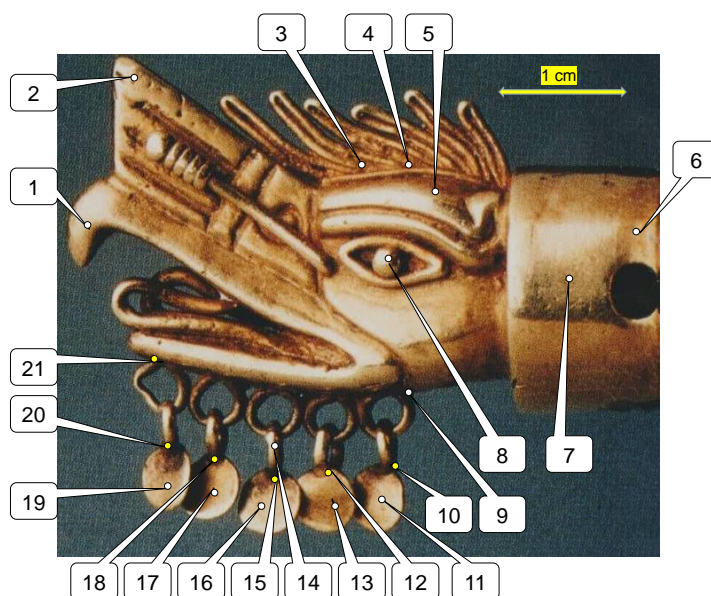
Twelve gold artefacts, displayed at “Europalia Mexico” exhibition held in Brussels in 1993 (Solis and Carmona-Macias 1993), were studied in collaboration with Martha Carmona Macias of the National Museum of Anthropology (Mexico City). Objects were excavated from tomb 7 of Monte Alban. They are attributed to the Mixtecs culture (Mexico). Mixtecs were the most skilled goldsmiths of Mesoamerica. Their civilization developed in the Oaxaca regions during the post-Classic period (from 900 AD until the conquest) and replaced the Zapotecs, the dominant culture during the Classic period in Oaxaca. About 80% of the existing Mesoamerican gold artefacts belong to the Mixtec tradition. The most important collections are in the Oaxaca Room of the National Museum of Anthropology (Mexico City), in the Museo de las Culturas de Oaxaca and in the Fisherman’s Treasure in the Baluarte de Santiago in Vera Cruz. The collection of MNAH is composed of artefacts from various regions of the Oaxaca area (the Central Valleys and the

Sierra): zoomorphic items, necklaces, rings and ear ornaments, bells, foils, etc. (Ruvalcaba et al. 1997). The most outstanding gold treasure of pre-Hispanic Mexico was discovered in 1934 at Monte Alban, in a tomb reused by the Mixtec people (Caso, 1969). In this multiple burial, artefacts made of green stones, turquoise, shells, bones, gold (121 artefacts) and silver were discovered (Ruvalcaba et al. 2009). Results on two chin pendants are discussed here.

Finest details are employed to simulate the threads of the serpent chin pendant (2.5 cm height 2.7 cm large and 4.5 cm thick) made by lost wax casting (figure 16). This lost wax technique was also used to produce granulations (false granulation) and mesh decorations (false filigree). PIXE results (in the non-vacuum configuration) at 21 impacts (Fig. 16) are shown in table 1. The concentration of Cu (3.2 %) is the same at all impacts even in the regions where some soldering could have been necessary (9, 12, 15, 16, 18, 20 and 21).

Table 1. Serpent chin data

impact	Gold	Silver	Copper	Remark
1	65,9	30,4	3,7	
2	65	32,7	3,3	
3	66,7	30,7	2,6	
4	67,1	29,9	3	
5	69,8	27,9	2,3	
6	64,3	32,5	3,2	
7	63,8	32,9	3,3	
8	64,9	31,8	3,3	
9	70,9	25,7	3,4	solder?
10	67,9	28,9	3,2	
11	65,4	31,3	3,3	
12	67,1	29,4	3,5	solder?
13	67,9	28,4	3,7	
14	64,3	32,5	3,2	
15	66,3	30,4	3,3	solder?
16	67	29,4	3,6	solder?
17	65,2	31,5	3,3	
18	66,6	30,3	3,1	solder?
19	65	32	3	
20	65,6	31,4	3	solder?
21	69	28,1	2,9	solder?

**Figure 16: Serpent chin pendant studied by non-vacuum PIXE**

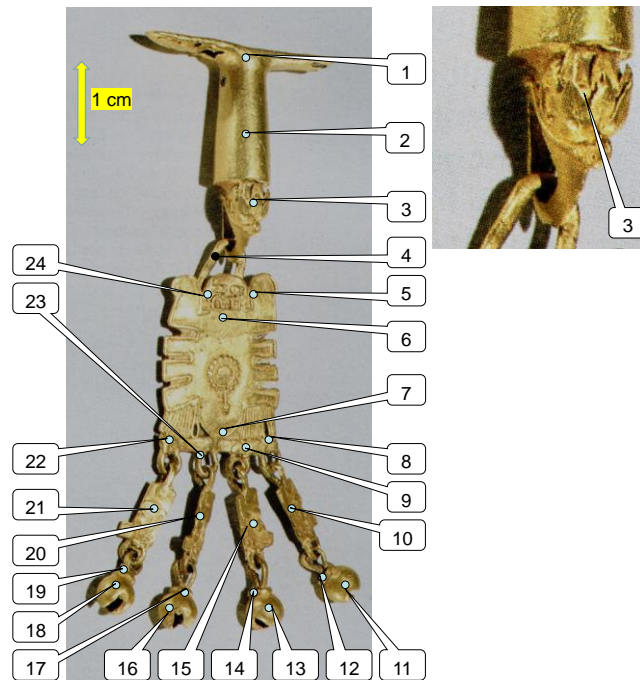


Figure 17: Eagles chin pendant studied by non-vacuum PIXE

The eagles chin artefact (Fig. 17) is also made by lost wax casting with two different alloys. In the upper part (impacts 1 to 4) including the eagles' decoration (impact 3) the composition is 78.8 ± 0.5 % Au, 17.1 ± 0.5 % Ag and 3.6 ± 0.4 % Cu while the rest of the item contains a lower concentration of gold: 66.7 ± 2 Au, 28.5 ± 3 % Ag, and 4.8 ± 1.3 % Cu. No solder can be observed in this eagles' chin ornament of figure 17 and data of Table 2. It is indeed often reported that no soldering technique was used by the Mixtec artisans (Bray 1978). Other more prestigious artefacts were studied during this thesis and later at the accelerator facility of UNAM (Mexico University).

Table 2. Eagles chin data

impact	Gold	Silver	Copper	Remark
1	78,5	18	305	top
2	78,4	17,7	3,9	top
3	78,4	18,3	3,3	top
4	79,9	16,2	3,9	ring
5	64,4	30,8	4,8	central
6	67,6	28,8	3,6	central
7	68,7	27,8	3,5	central
8	66,9	28,1	5	central
9	65,8	29,5	4,7	central
10	64,6	30,3	5,1	strip 4
11	67,2	28,1	4,7	sphere 4
12	64,9	30,4	4,7	solder?

13	69,6	25,6	4,8	sphere 3
14	66,5	27,8	5,7	solder?
15	67,3	26,9	5,8	strip 3
16	69,8	25,7	4,5	sphere 2
17	66,1	27,7	6,2	solder?
18	66,6	28,8	4,6	sphere 1
19	66	29,3	4,7	solder?
20	66,7	28,1	5,2	central
21	67,3	28,1	4,6	strip 1
22	65,8	29,4	4,8	central
23	64,9	30,1	5	central
24	65,7	29,4	4,9	central

4. SOPHISTICATE JEWELLERY OF ACHAE-MENID EMPIRE

Pierre Amiet, the former curator of the Department of Oriental Antiquities of Le Louvre museum was very enthusiast to allow the transportation of several prestigious objects of his collection for their analysis outside France, well before the installation AGLAE in Paris. Among the numerous items of ancient Achaemenid Empire studied at LARN, the "Bes" pendant (IVth-VIth century BC) of Fig. 18 (Louvre museum - AO 3171) brings a brilliant demonstration of Iranian goldsmith's know-how (Demortier 1991a).

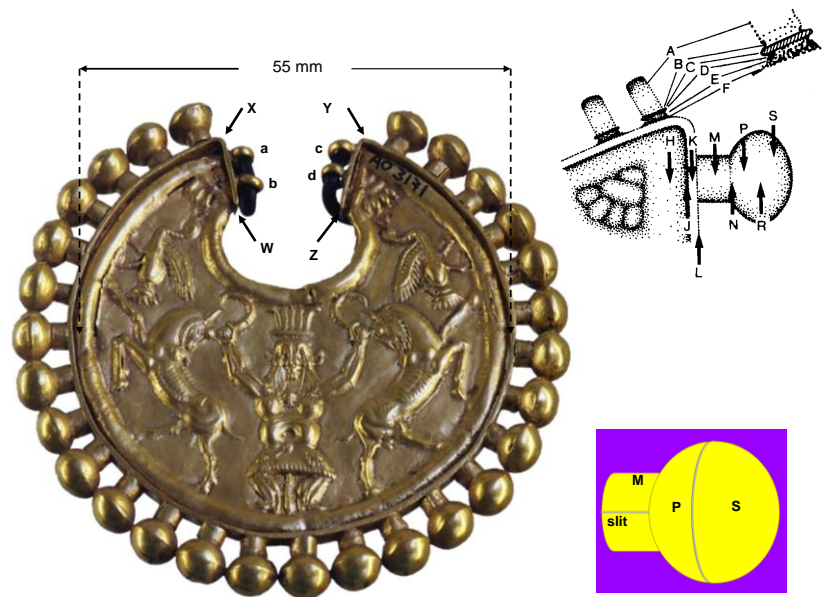


Figure 18: Acheamnid pendant studied by PIXE-microprobe

The central part (diameter 5.5 cm) is made with 2 identical disks for front and back faces. Disks are decorated by the “repoussé” (hammered) process with Egyptian God “Bes” subduing two goats topped by two birds.

From non-vacuum PIXE analysis at various places it is certified that both “Bes” disks are made with a homogeneous alloy: $81 \pm 3\%$ Au, $14 \pm 1\%$ Ag and $5 \pm 1\%$ Cu. The strip maintaining the decorated disks (from W to Z) has the same composition. The surrounding decoration is made with 28 decorative elements, all identical, made each in 3 parts: one cylinder 1.8 mm high (with lateral open slit) and 3 mm in diameter, two nearly hemispheric cups with a diameter of 6 mm for a maximum length of 8 mm of the whole composition. The 4 loops (a, b, c, d) are made with some other gold alloy (74% Au) and could have been added for modern convenience.

The artefact was also studied in the nuclear microprobe configuration of Fig. 9. The item was fixed on an X-Y frame to be moved in the proton beam ($5\ \mu\text{m}$

spots) by computer controlled stepping motors allowing mechanical displacements whose position can be reproduced with great accuracy (better than $2.5\ \mu\text{m}$ after translation of several centimetres). The collected PIXE data at 125 impacts over a distance of only 12 mm are given in Fig. 19. Four regions requiring a soldering procedure have been identified at J, L, N and R. Both concentrations of Cu and Ag in regions J and L are higher than in the surroundings indicating that copper and silver ores have been added to the basic gold alloy to obtain a new alloy with a lower melting temperature for brazing use. The relative concentrations of Au, Ag and Cu at impact N and R does not refer to this usual criterion: one observes a drastic increase of Au (about 8%) in the region N (contact of the cylinder M with the hemispheric part P) and consequently an associated decrease of both Ag and Cu. Such high gold concentration could be the consequence of a welding procedure without the addition of any additional material.

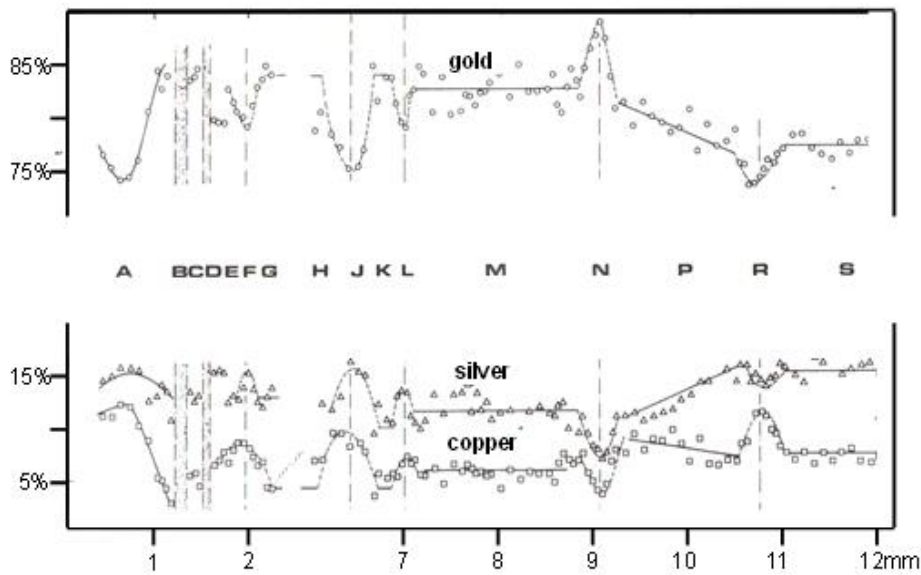


Figure 19: Gold, silver and copper concentrations in the Achaemenid pendant

The relative concentrations of Au-Ag-Cu at point N imply that end of cylinder M in contact with the hemispherical cup P was heated to an early stage of fusion. In this process, metals like copper and silver are selectively eliminated at the junction, mainly by oxidation, so that gold content is enhanced. The working temperature was around 1000 °C. At site R, an increase of copper concentration is observed with a decrease of both gold and silver. The two hemispheric caps P and S, previously mechanically well-fitted, were joined by the process known as solid-state diffusion bonding with copper salts in a reducing atmosphere. The process takes place at about 890°C. That soldering process was rediscovered and fully described by Littledale (Littledale 1936). This process gives rise to some solid phase that cannot be unsoldered by reheating: any temperature increase would allow copper to diffuse further in both parts of the junction with a resulting increase of the melting point. This temperature (890°C) is below that achieved at N

for the joining of M to P, and is not high enough to destroy the previous solder at N. The measured composition at L and J with increases of Cu and Ag for the joining of the 28 ornaments may be explained by the usual brazing process at $\pm 840^{\circ}\text{C}$ at L (to attach each external element to the external part of the strip) and finally at $\pm 820^{\circ}\text{C}$ for the joining at J of the whole decorated assembly to the "Bes" decorated disks.

The successive steps of manufacture of this wonderful jewellery of the IVth century BC is summarized in Fig. 20: (a) joining of each little cylinder to its adjacent hemispherical cap at 1000°C, (b) joining of the second hemispherical cap at 890°C. These procedure is repeated 28 times for each ornament, (c) joining of each of these ornaments to the strip (probably in flat position), (d) chain welding of the 28 elements giving rise to some unavoidable misalignment of the open slits, (e) repeated soldering for all the elements (840°C), (f) bending and soldering (820°C) of the whole decorated strip on the "Bes" disks.

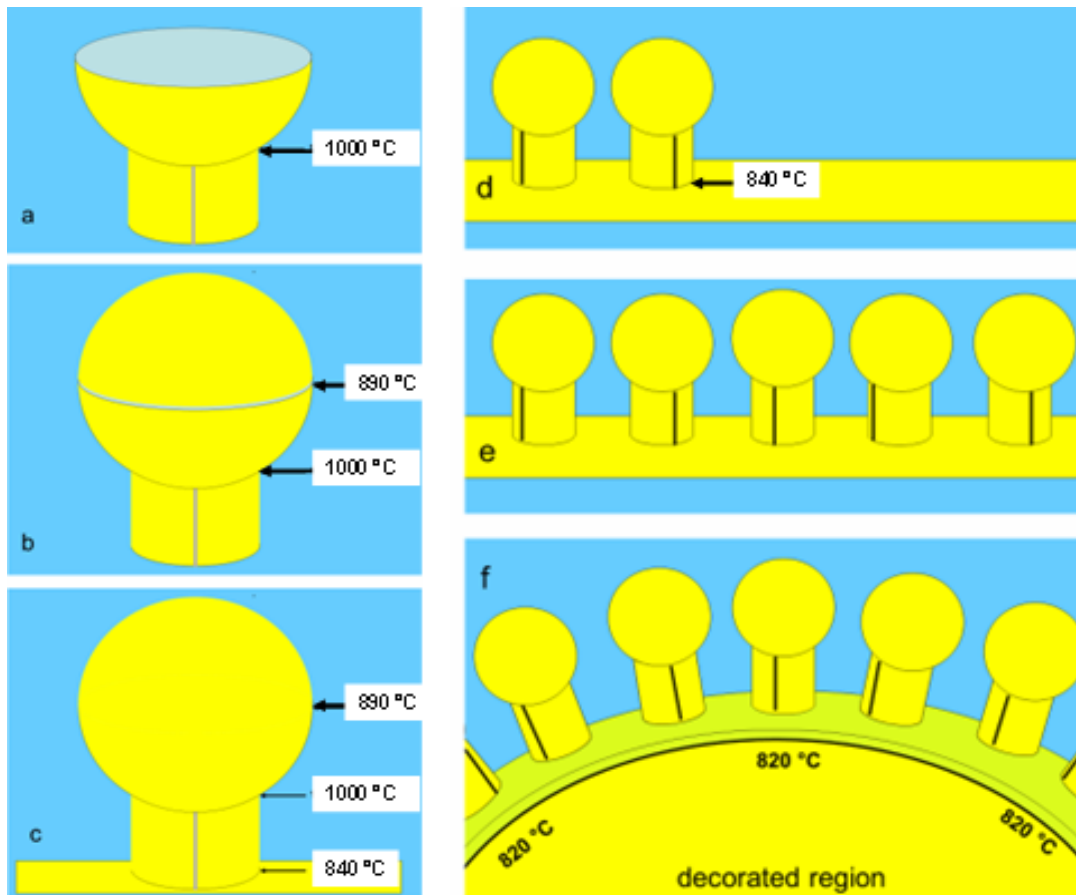


Figure 20: The 6 steps of soldering procedure in the Achaemenid pendant

Relative concentrations measurement of Au, Ag and Cu in a gold artefact is the best way to recognize which soldering process has been used.

5. GENUINE ARTEFACTS, RESTAURATED ITEMS OR FAKES IN ANCIENT IRANIAN JEWELLERY?

Gold jewellery items presented in the present review were studied on demand of museum curators in collaboration with recognized archaeologists. Based on their prior examination with traditional instruments in their own department, they recognize the artefact as genuine, except in some limited region where

a possible restoration could have been performed. The potential regions of restoration were always indicated prior any analysis. With this statement the analytical physicist and the archaeologist, who worked together at the accelerator facility, can stay in their own skill. Together they choose locations where an analysis is pertinent.

The rectangular Byzantine cover book (19 cm x 14 cm) of Fig. 21 was discovered (before 1946) by a French archaeological team in the region of Selemieh (Syria) and is the property of the Staatliche Museen Berlin (inv.A/60) (Elbern 1965).

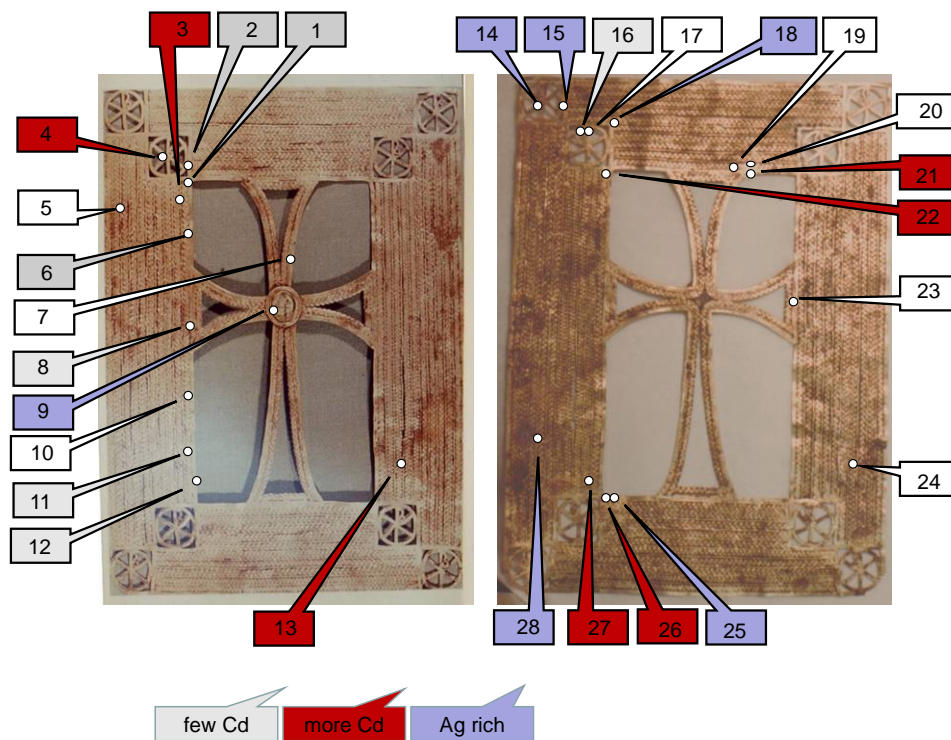


Figure 21: The Byzantine cover book of Berlin Museum

Similar artefacts are kept in Seattle Museum, Cleveland Museum of Art, Victoria and Albert Museum in London. The cover book is made from braided solid wires forming a cross in the centre which holds a bezel probably reused with its setting from some other jewel. At the four corners flat gold strips form two chrismons inserted in a square (see detail in Fig. 22). These ornaments interrupt the ten strips of braided wires which are attached to each other by beaded wires and form the rectangular surrounds of the cover. A detail around a chrismon clearly shows the structure of the surface with solder regions and traces of hammering of the braided wires. The cover book was technically studied by Artur Kratz (Kratz 1972) who was aware of the presence of cadmium in numerous regions.



Figure 22: Chrismon in the Byzantine cover book showing traces of hammering of wires

The presence of cadmium in ancient artefacts is still a problem of debate and several scholars are profoundly convinced that artefacts containing cadmium are fakes or repaired items. They declare that the detection of cadmium in on single region of the object is a criterion of rejection (Meeks and Craddock 1991). The problem is not so simple (Demortier 1991b). The presence of cadmium is not the unique criterion to reject the authenticity of an ancient artefact. Accepting or rejecting a genuine artefact requires more information: mainly the relative concentrations of Cu, Ag and Cd in the gold alloy and incidentally the concentration of Zn and other light elements (i.e. Al, Si, S) associated with the origin of cadmium ores (see discussion below).

Non-vacuum PIXE results on the cover book are given in Table 3. Front face is very gold rich (about 97.5% except for the central bezel setting (impact 9: 80.9% Au) but the rear face is less gold rich and highly non-homogeneous. Cadmium is found in 12 analysed regions. After subtracting the contribution of Au the relative concentrations of Cu-Ag-Cd are displayed in the ternary diagram of Fig. 23. The data are scattered along the arrow pointing to the “100% Cd corner”: along this arrow the ratio Ag/Cu does not change. In every ternary diagram (Cu-Ag-Cd) the arrow direction points to the region of highest Cd concentration.

Table 3. Byzantine cover book data

	Front				remark
impact	Gold	Silver	Copper	Cadmium	
1	98,9	0,25	0,61	0,23	
2	98,55	,047	0,62	0,36	
3	98	0,55	0,52	0,92	
4	97,8	0,3	0,35	1,55	
5	99,15	0,38	0,48		
6	98,15	0,75	0,92	0,18	
7	95,3	3,05	1,65		
8	98,25	0,8	0,95	0,05	
9	80,95	16,5	2,57		bezel
10	98,7	0,55	0,8	0,03	
11	98,85	0,55	0,55	0,03	
12	98,15	0,56	1,3		
13	92,2	3,3	3,35	1,15	Ag-Cu-Cd
		Back			
14	82,4	9,75	7,85		high Ag+Cu
15	73,7	8,7	17,6		
16	99,55	0,15	0,25	0,05	
17	99,9		0,03		very pure Au
18	46	31	23		strange
19	85,55	5,15	9,3		
20	84,2	5,4	10,4		
21	82,9	5,5	10,8	1,2	
22	69,7	7,85	21,6	0,85	high Ag
23	79	8,1	12,9		
24	87,7	5,4	6,9		
25	76	10,25	13,75		high Ag+Cu
26	94,15	1,5	3,05	1,3	
27	97,4	0,6	0,65	1,35	
28	83,09	7,95	8,15		high Ag+Cu

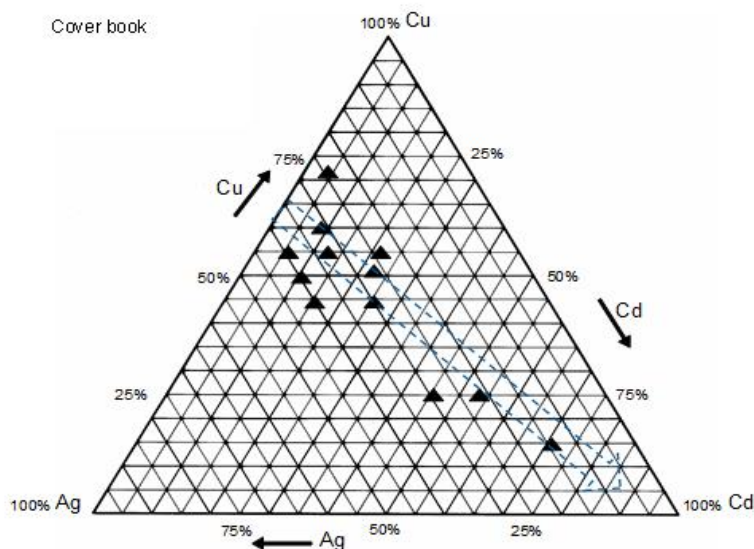


Figure 23: The ternary diagram of Cu-Ag-Cd of the Byzantine cover book



Figure 24: The Roman necklace of Flavian Emperors (1st century AD)

A necklace of loop-in-loop type belonging to a private collection is shown in Fig.24. The finials of the three-link column chain (66 cm long) are covered by a cap to which a small loop is attached on both sides, one of them holding a rather large hook. On this chain are threaded 5 medallions kept at a suitable distance by mobile elements decorated in the repoussé technique with a spiral motive. The 5 gemstones have the portrait of Vespasian (centre), Titus (left of Vespasian), Domitius (right of Vespasian), Julia Titi (daughter of Titus at far left) and Domitia (wife of Domitius at far right); they are displayed in Fig. 25 and their back side in Fig. 26. Each stone is set in a flat gold foil

decorated on the sides by a series of granulated triangles, surrounded by another strip affecting a wavy "ajouré" line. Other smooth filigree holds the exterior circle with a slightly twisted strip attached to it. A grape of hollow spheres, with small granulations, is fixed on the twisted strip beneath each portrait.

The portraits suggest that the whole set was made in the very early years of the Vespasian's reign, as numismatic parallels show. The Palestinian provenance of the necklace (first century AD) may connect the piece with the Flavian successes against the Jews in that area.



Figure 25: Front faces of the Roman necklace of Flavian Emperors (1st century AD)

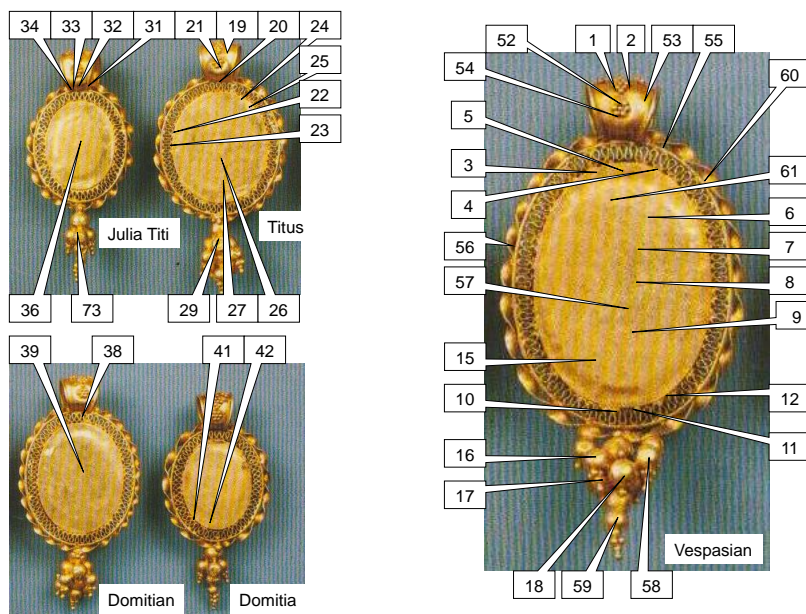


Figure 26: Rear faces of the Roman necklace of Flavian Emperors (1st century AD)

Non-vacuum PIXE results collected at 80 locations are given in Table 4. Special attention has been taken in the regions where a soldering process could have been applied (at 38 on the 80 impacts). The ternary diagram of Cu-Ag-Cd is shown in Fig. 27 with 4 differ-

ent colours corresponding to the absolute Cd concentrations (0.1 to 0.5%; 0.5 to 1%; 1 to 5%; 5 to 10%). All the data are scattered along a region starting from the Ag 100% corner: the Cd concentration increases proportionally to the Cu one. This behaviour is opposite to that observed for the cover book.

Table 4. Roman necklace data

impact	Au	Ag	Cu	Cd	comment
1	94,8	2,8	1,9	5	granule
2	95,25	2,9	1,5	0,35	granule
3	84,35	1,3	9,2	5,1	solder
4	83,55	1,4	9,75	5,3	solder
5	96,1	3,1	0,8		
6	95,7	3,3	1		
7	96	3,3	0,7		
8	96,2	3	0,8		
9	96,1	3,2	0,7		
10	95,25	3	1,9	0,85	solder
11	96,25	3	0,6	0,15	serpent
12	95,7	3	1	0,3	serpent
13	95,7	3,4	0,6	0,7	cup Vesp
14	93	2,5	3,2	1,3	serpent
15	94,45	3,3	1,8	0,45	cup Vesp
16	94,6	2,9	1,8	0,7	globule
17	93,95	3	1,6	0,45	globule
18	96	2,9	1	0,1	globule
19	93,35	2,9	2,2	0,75	granule
20	80,25	0,2	10,85	8,7	solder
21	80,2	1,4	9,85	7,9	granule
22	93,25	1,9	3,4	1,45	serpent

23	92,2	3,3	3	1,5	serpent
24	94	3,3	2	0,75	serpent
25	91	3,5	3	2,5	serpent
26	96	3,2	0,8		
27	96,2	3	0,8		
28	87,8	2,3	6,9	2,9	?
29	96,3	3,2	0,5		
30	95,2	3,1	1,1	0,6	?
31	95,55	3	1	0,45	serpent
32	83,2	1,2	10,1	5,4	serpent
33	82,45	1,5	9,3	6,75	serpent
34	78,6	1,1	11,8	8,6	serpent
35	93,45	3,6	2,8	0,15	?
36	96,2	3,1	0,7		
37	88,2	3,,1	3,2	5,4	?
38	80,3	0,65	13,5	5,5	serpent
39	95,8	3,1	1,1		
40	80,8	1,35	12,95	4,85	?
41	92,3	3,6	2,9	1,2	
42	95	3	1,4	0,6	
43	95,25	3,3	1,1	1,35	
44	92	2,7	2,1	3,2	
45	95,9	3,2	0,9		
46	95,7	3	1,3		
47	95,7	3,4	0,9		
48	95,9	3	1	0,1	
49	96,3	3,1	0,6		granule
50	96	3,1	0,9		cap
51	96,1	3,1	0,8		globule
52	96,2	3	0,8		granule
53	96,2	3	0,8		beliere
54	95,5	3,1	1,4		granule
55	96,4	3	0,6		serpent
56	96,3	3	0,7		serpent
57	96,1	3,2	0,7		cup vesp
58	95,8	3,5	0,7		globule
59	96,2	3	0,8		globule
60	96,2	3	0,8		serpent
61	96,1	3,1	0,8		cup vesp
62	96,2	2,9	0,9		?
63	96,3	3	0,7		?
64	95,8	3,3	0,9		granule
65	95,5	3,5	1		cup Titus
66	96	3,2	0,8		cap Titus
67	95,8	3,2	1		granule
68	96,2	2,9	0,9		cap Donatian
69	95,8	3,1	1,1		cap Donatian
70	95,2	3,1	1,7		cap Donatian
71	95,9	3,3	0,8		torsade
72	96	3,2	0,8		granule
73	94,7	4,6	0,7		
74	95,5	3,3	1,2		granule

75	96,1	3,2	0,7		
76	95,6	3,4	1		globule
77	96	3	0,8		serpent
78	89,9	2,9	3	4,1	?
79	90,9	2,6	2,4	4,1	?
80	90	2,75	2,6	4,7	?

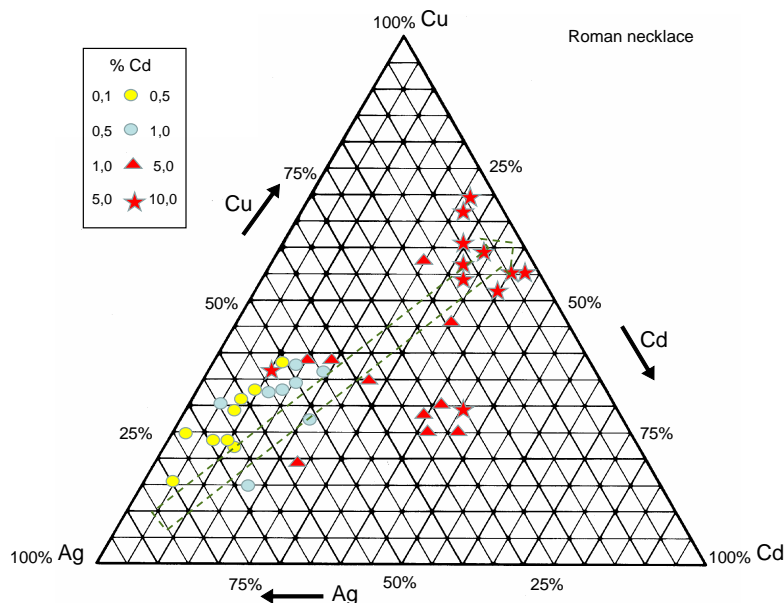


Figure 27: The ternary diagram of Cu-Ag-Cd of the Roman necklace

5.1 Cadmium in ancient gold jewellery and experimental archaeology

Whilst studying compounds of zinc carbonate, Friederich Strömeyer, senior inspector of pharmacies in Hanover, discovered cadmium as a new element (in 1817). Cadmium is a common impurity of naturally occurring zinc compounds, though often found only in minute quantities. Cadmium has been widely used in jewellery shops, by the end of the 19th century, as it confers good melt fluidity as well as lowering the melting range. Metallic cadmium has a low melting point (321°C) and boils at 767°C. Unfortunately, metallic cadmium is also known for its serious toxicity and is now prohibited in numerous countries.

This late identification of cadmium as a new chemical element by Strömeyer (in 1817) cannot be recognized as a proof that it was not used before. It could have been appreciated by ancient goldsmiths on the basis of the colour of its natural occurrence (CdS) which is very close to the colour of gold, well before Strömeyer gives it a name. Cadmium ores are present in soil since the birth of the earth!

Ancient metallurgy could be called ancient "mineralurgy": ancient alloys were indeed created by the action of fire directly on ores which contain the metal and not by alloying their metallic form.

Experimental archaeology was therefore undertaken in LARN by using natural ingredients only. Cadmium supply could be natural cadmium sulphide or greenockite (identified in 1840 by Lord Greenock in Scotland). CdS is notably present as a yellow coating on a zinc blend (Fig. 28a and 28b). Hexagonal mesh CdS may be easily removed from its zinc blend support which is a face-centred cubic mineral. The colour of greenockite is very similar to that of gold. With a high melting point (980°C) greenockite does not violently react when mixed in molten gold or gold rich alloys. On the contrary pure cadmium straw dropped into molten gold (as made with the utmost care in goldsmith's shops) gives off black smoke and induces great cadmium loss.

Grains of greenockite were deposited on several Au-Ag-Cu (but Cd free) alloys. When heated in a charcoal vessel up to 600-700°C (below the Cd boiling point) one obtains a sphere of alloy with partly some earthy aspect (Fig. 28c). When the sphere is laminated the earthy part is eliminated leaving a metallic structure (figure 28d) with various colorations. This alloying operation was repeated with different copper contents (2%, 4% and 12%) in gold. Relative concentrations of Ag-Cu-Cd in laminated foils measured with PIXE are reported in the ternary diagram of Fig. 29.

Cadmium rich regions coincide with copper rich regions. This behaviour was compared with that of commercial quaternary alloys (Au-Ag-Cu-Cd). The results of (Ag-Cu-Cd) distribution are given in figure 30. When heated up to the first step of fusion cadmium is partially eliminated (due to its low melting

point) but the relative concentration of Ag and Cu is maintained (red stars in figure 30). When used to braze, Cd elimination progresses but the Ag/Cu ratio stay unchanged (yellow circles in Fig. 30).

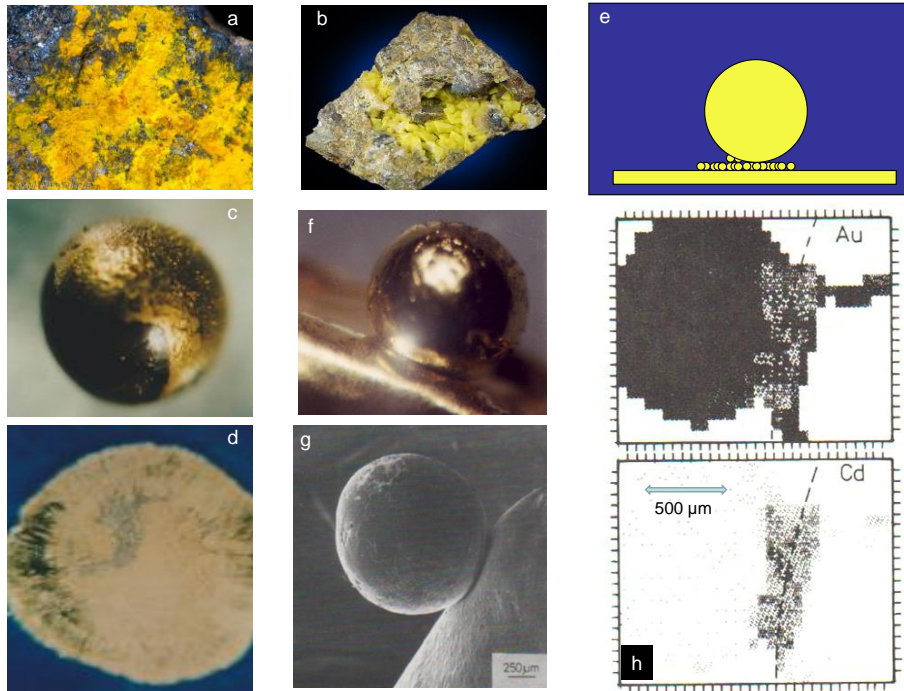


Figure 28: Experimental archaeology using greenockite

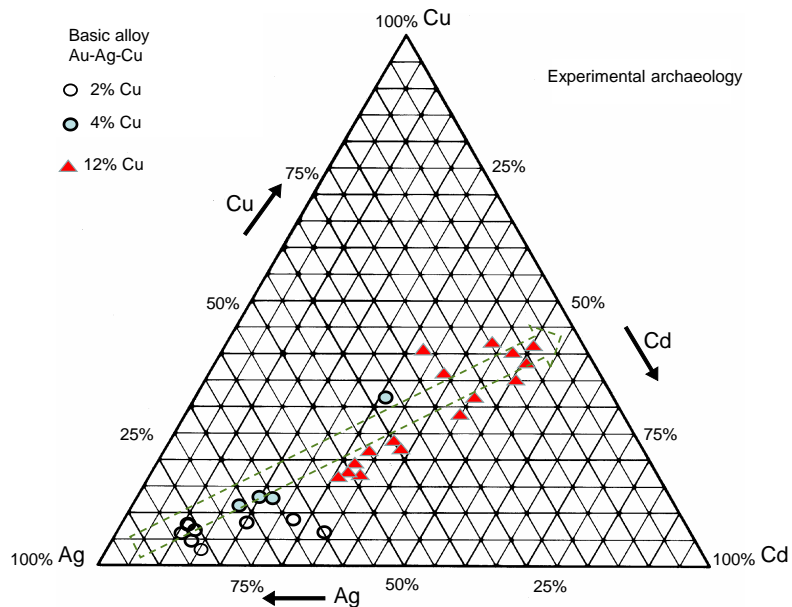


Figure 29: The ternary diagram of Cu-Ag-Cd of alloys made with greenockite

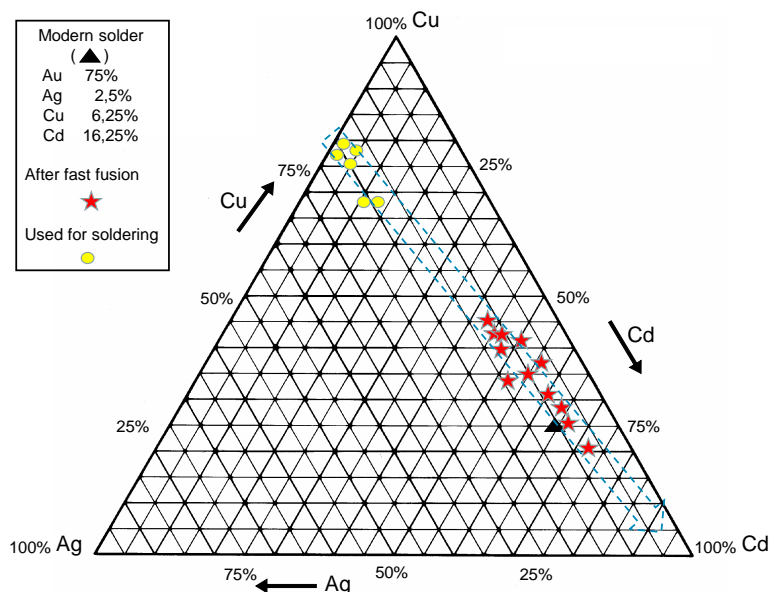


Figure 30: The ternary diagram of Cu-Ag-Cd of a modern soldering alloy

Granulation is easily realized by absorption of Cd from grains of greenockite in gold: a gold granule of 1.5 mm in diameter (Fig. 28e) was deposited on a sheet of gold (spread with CdS powder) and heated up to 700°C. The result showing a clean joining is presented in Figs. 28f and 28g (optical and electron microscopes). This soldered granule and its gold sheet support were cut along the sphere diameter and analysed with the PIXE-microprobe to scan the soldered region (Fig. 28h). Migration of Cd is observed up to 100µm on both sides of the join. The result is very similar to that obtained by Cu diffusion bonding already shown in the decoration of the Achaemenid pendant (Litteldale 1936) but at a lower temperature with CdS. The full description of this simultaneous alloying and brazing process “by soft minerallurgy” may be found in works of Decroupet and Mathot (Decroupet et al. 1989).

5.2 Cu-Ag-Cd behaviour in Byzantine cover book and Roman Necklace

The Byzantine cover book and the Flavian necklace (and also numerous other artefacts) were presented to analytical physicists for non-destructive analytical investigation by distinguished art historians who had no a priori doubt on their authenticity, they have been

already studied with usual optical or electron microscopy in their own institute. Very often also these art historians were surprised when cadmium was discovered.

If greenockite is the origin of Cd in solders of a gold artefact, it could be expected that traces of S and/or Zn would be also present in the regions of solders: greenockite is indeed a sulphide which would have been scratched from a zinc blend. Unfortunately the Roman necklace did not stay in the laboratory long enough (due to security and insurance requirements) to perform additional S and Zn measurements. Nevertheless artefacts of lower value which were discovered in the excavation site with the necklace were longer available and studied with the appropriate nuclear reaction set-up for (d,p) analysis of S (same as figure 9) simultaneously with PIXE induced by the deuteron beam and also with the XRF induced by PIXE set up (Figs. 11 and 12).

The artefact (Fig. 31-(1)) is a small gold hollow sphere (12 mm in diameter). PIXE- microprobe results on the selected part (a) of a 5 mm wide region are given in part (31-2). Due to the rounded relief of the surface, shadowing effect could affect the detection of X-ray signal of all elements (noted s). This effect is partially corrected if the local content of Cu, Ag and Cd is divided by the Au content as shown in part (Fig.31-3).

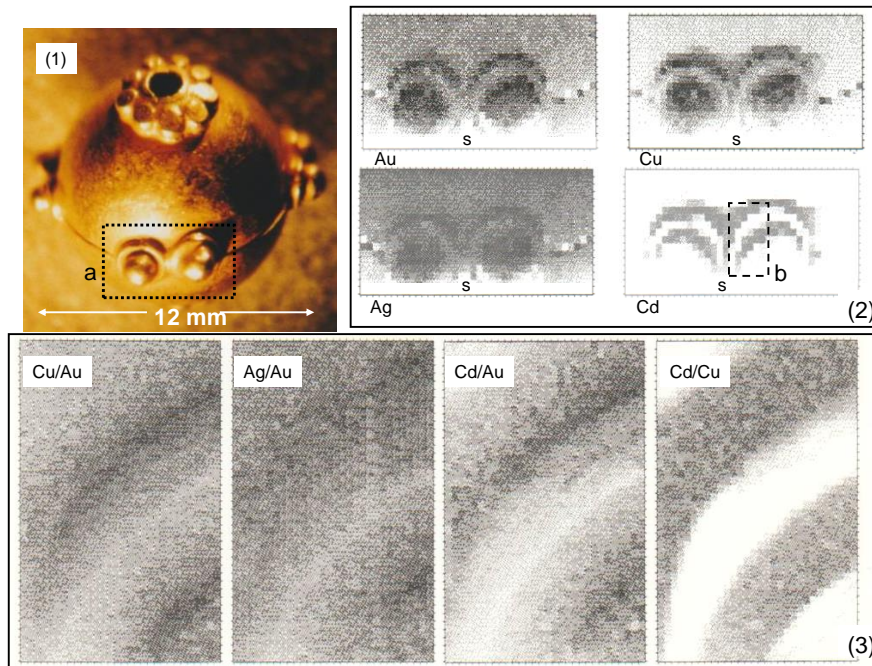


Figure 31: Soldering regions of a gold hollow sphere studied with the PIXE microprobe

Strong correlation of Cu/Cd is quite evident. Traces of Zn (100 to 200 ppm) were also observed in the small gold hollow sphere by XRF induced by PIXE at concentration well below that of Cd. Zinc could be an additional metal in modern Cd-based soldering alloys but with a ratio Zn/Cd of the order of 20-30%. Traces of Zn in the hollow sphere are then not of modern origin.

Clusters of data around the 100% Cd corner in a ternary diagram of Fig. 23 related to the Byzantine cover book (similar to that of figure 30 for modern Cd based solders) is a sign of recent goldsmith work. This fact has been already announced with other arguments by A.Kratz (Kratz 1973).

The absence of data around the 100% Cd corner in Fig.27 (Roman necklace) but mainly the similitude in the slope of the arrows of Fig.29 would indicate that the artefact is not modern. The ancient workmanship

of the whole necklace was expected by the art historian who was confident on its authenticity before the metal was analysed, on the basis of his expertise in the work on each of the gems (their cut, their polish, their settings in full agreement with ancient technologies). Observed by optical microscopy, it was demonstrated that the 5 gems were never removed from their original gold settings.

The presence of Cd in a Hellenistic golden funerary belt was recently reported by Alicia Perea (Perea et al., 2018). The announced concentrations of Ag, Cu and Cd in 6 regions of the artefact are introduced in a ternary diagram (Fig. 32). The distribution of Cu-Ag-Cd relative concentrations shows a strong correlation of Ag/Cu and no contribution in the high Cd area (bottom left corner). No use of modern brazing alloy containing cadmium has been applied on this Hellenistic item.

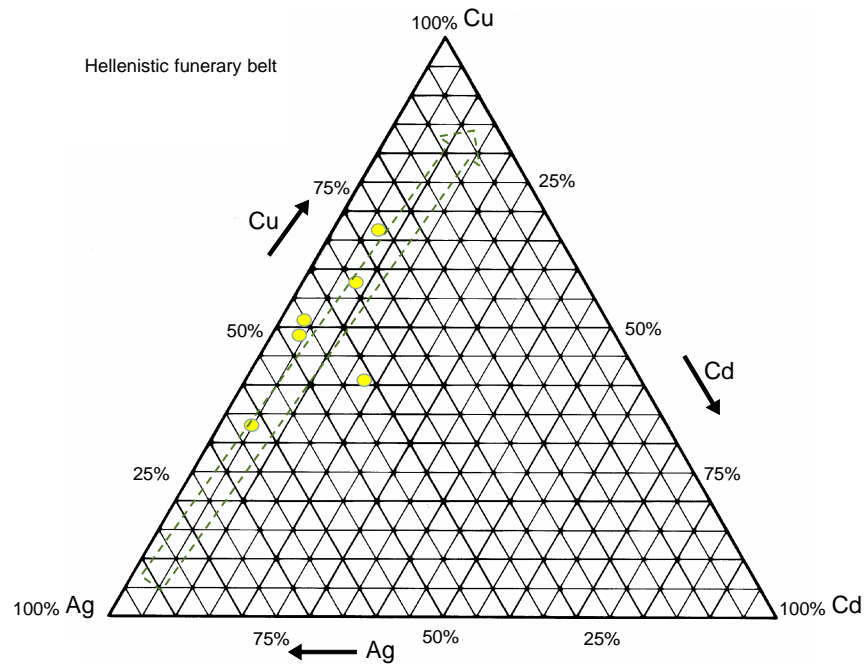


Figure 32: The ternary diagram of Cu-Ag-Cd of the Hellenistic funerary belt (Perea 2018)

6. ANCIENT GOLD SOLDERING: WHAT IS CHRYSOCOLLA?

What is really chrysocola ($\chi\rho\upsilon\sigma\omicron\kappa\omicron\lambda\alpha$)? The answer is perhaps given in Pliny's "Natural History" (Zehnacker 1983)

The description of technological aspects in the encyclopaedic work of Elder Pliny starts only with Liber XXXIII. The first subject concerns mining technology. In the introduction: "We are now about to speak of metals, of actual wealth, the standard of comparative value, objects for which we diligently search, within the earth, in numerous ways...we undermine it for the purpose of obtaining riches". Directly after the introduction he writes in the second paragraph: "Gold is dug out of the earth, and, in close proximity to it, chrysocola" (concisely written in the Latin version to state the importance of chrysocola in gold technologies "eruitur aurum et chrysocola iuxta") a substance which, that it may appear all the more precious, still retains the name which it has borrowed from gold. It was not enough for us to have discovered one bane for the human race, but we must set a value too upon the very humours of gold". In the next 24 paragraphs Pliny continues to stick to the negative aspects of gold utilization and he only gives it value for medical applications.

Technical applications of chrysocola firstly concern its use as colorant (paragraph 26). Let us read it in the Bambergensis version of the manuscript (10th century) "Native chrysocola, known as "uva," differs from the other in its hardness more particularly; and yet, hard as it is, it admits of being coloured with the plant

known as "lutum.". The translation of the term "uva" often refers to the "shape" of native chrysocola which is then identified to malachite whose shape could evoke that of grape: malachite is a copper ore with a green colour and not a yellow colour like "lutum". In the original Latin version: « *Nativa durita maxime distat; uam uocant. Et tamen illa quoque herba, quam lutum appellant, tingitur* », no evidence to the shape of chrysocola could be found. Chrysocola is "uva" but Pliny immediately adds insistently "Et tamen" ideally translated by "And nevertheless" it is dyed with a plant to become more pronounced with a yellow colour.

In the Parisinus Latinus version of Pliny's Natural History (13th century) "uva" is replaced by "luteam" which clearly refers to yellow, orange or golden. If chrysocola refers to some property of grape the said property would qualify the colour of mature golden grape but not immature green grains (Demortier 1987b).

The most important argument concerns the goldsmith's use of chrysocola (paragraph 29).

"The goldsmiths also employ a chrysocola of their own, for the purpose of soldering gold; and it is from this chrysocola, they say, that all the other substances, which present a similar green, have received their name."

The Bambergensis Latin version of the bolt sentence is "et inde omnis appellatas similiter uirentes dicunt". "Uirentes" could be certainly translated as "verdant" but also as "shiny". In the Parisinus Latinus version "uirentes" is replaced by 'utentes'.

"This preparation is made from verdigris of Cyprian copper, the urine of a youth who has not arrived at puberty, and a portion of nitre. It is then pounded with a pestle of Cyprian copper, in a copper mortar, and the name given to the mixture is "santerna."

Santerna could fit with the description of malachite but the following additional caution is very scheming: *It is in this way that the gold known as "silvery" gold is soldered; one sign of its being so alloyed being its additional brilliancy on the application of santerna. If, on the other hand, the gold is impregnated with copper, it will contract, on coming in contact with the santerna, become dull, and only be soldered with the greatest difficulty: indeed, for this last kind of gold, there is a peculiar solder employed, made of gold and one-seventh part of silver, in addition to the materials above-mentioned, the whole beaten up together".*

It is known today that alloying Au with Ag and Cu is feasible in all proportions. Why might copper rich gold alloys be refractory to be soldered with any copper ore? The answer it to be found in the experimental archaeology check of figure 28c: earthy deposit takes place in the alloying procedure of greenockite with melted copper rich gold alloy (Demortier 1987b, Demortier 1989)

ACKNOWLEDGMENTS

Numerous people were involved in this analytical research on gold artefacts which started in 1980. Many thanks to physicists and technical staff involved in the construction and management of the analytical equipment: G. Deconninck, Fr. Bodart, Y. Morciaux, M. Piette, B. Van Oystaeyen and Y. Houbion (University of Namur), G. Quarta and L. Calcagnile (CEDAD - Salento University), Z. Smit (Ljubljana University), M.-F. Guerra (AGLAE Paris) and J.-N. Barrandon (CNRS Orleans).

Warm thanks also to art historians and museum curators who agreed to entrust us with prestigious jewellery items : Late T. Hackens (University of Louvain- Belgium), G. Nicolini (University of Poitiers - France), Pierre Amiet (Antiquités Orientales of Le Louvre Museum Paris- France), V. Elbern (Staatlichen Museen Preußischer Kulturbesitz Berlin - Germany), R. Van Laere (Koninklijk Belgisch Genootschap voor Numismatiek Tongeren - Belgium), J. Dumoulin (Trésor de la Cathédrale de Tournai - Belgium), J. Bienaimé (Musée Archéologique de Troyes - France), R. Winkes (Brown University Providence - USA), M. Carmona Macias (Museo Nacional de Antropología Oaxaca - Mexico), A. Perea (CCHS-CSIC, Madrid), F. Fernandez-Gomez (Archaeology Museum Seville - Spain), S. Bobomulloev (National Museum of Antiquities of Tajikistan).

Ph.D. students D. Decroupet, S. Mathot and J.-L. Ruvalcaba-Sil and master students F. Van Haemelrijk, A. Gilson, A. Boullar, C. Vermeyen-Moor, C. Steukers, N. Vandesteene, D. Dozot, P. Coquay (University of Namur- Belgium), M. Ontalba-Salamanca (University of Seville - Spain) have actively contributed to measurements, bibliographical research and fruitful discussions.

REFERENCES

- Amsel G., Heitz Ch., Menu M. (1986). MeV ion beam techniques: an outline, *Nuclear Instruments and Methods in Physics Research*, B14, pp. 30-37.
- Bray W., (1975) *Gold working in ancient America* - Gold Bulletin 11(4), pp. 136-143.
- Bray W., (1993) Techniques of gilding and surface enrichment in pre-Hispanic American metallurgy. In: *Metal Plating and Patination*, S. La Niece and P. Craddock eds., Butterworth Heinemann, Oxford, pp. 182-192.
- Callister W. D. Jr, (2000) *Materials Science and Engineering, An Introduction*, John Wiley & Sons Inc, U.S.A

7. CONCLUSIONS

PIXE, RBS and NRA are powerful tools for the analytical study of ancient gold artefacts. The techniques are non destructive even for fragile materials. The simultaneous detection of characteristic X-rays of all elements present in the artefact by non-vacuum PIXE gives the widest panoramic analysis. When PIXE is combined with RBS, ideally in the microprobe configuration, depth profile may contribute to obtain quantitative information on potential surface treatment. XRF induced by PIXE, nuclear reactions induced by a deuteron beam and gamma-ray transmission for the exploration of hollow may bring complementary information. Pre-Hispanic American and ancient Iranian gold artefacts have been selected amongst the numerous objects studied at LARN (Namur University) to demonstrate the performances of the analytical tools. Comparison between old and new soldering techniques is extensively studied. In addition to material analysis experimental archaeology was performed for the reconstitution of depletion gilding and for alloying gold with golden coloured ores to obtain low melting point gold solders. A non-conventional view of the meaning of chrysocola (Χρυσόκολα) is proposed.

- Caso A., (1969). *El Tesoro de Monte Albán*. Memorias del Instituto Nacional de Antropología e Historia III. México: Instituto Nacional de Antropología e Historia
- Cohen D.D., Harrigan M., (1975) *K- and L-shell ionization by p and He* Atomic data and nuclear data tables, 34, pp. 255-343.
- Deconninck G. (1972) Quantitative analysis by (p,X) and (p, γ) reactions at low energy, *Journal of Radioanalytical Chemistry* 12, pp. 157-169
- Deconninck G. (1978) Introduction to Radioanalytical Physics, *Nuclear Methods Monographs* 1 Elsevier
- Deconninck G. and Demortier G. (1975) *Thick target excitation yields of prompt gamma radiations from proton bombardment of Rh, Pd, Ag, Pt and Au* Journal of Radioanalytical Chemistry 24, pp. 437-446.
- Decroupet D. and Demortier G. (1988) *Solid state bonding using cadmium diffusion* Proc.Int.Conf. on Hot Isostatic Pressing of Materials: applications and developments. Antwerp 3, pp. 19-22.
- Decroupet D., Mathot S., Demortier G. (1989) Diffusion bonding of gold using microscopic Au-Cd alloys, *Journal of Materials Sciences Letters* 8, pp. 849-851.
- De Cuyper F., Demortier G., Dumoulin J., Pycke J. (1987) *La croix Byzantine de la cathédrale de Tournai* Aurifex 7, Université Catholique de Louvain.
- Demortier G. (1981) The soldering of gold in Antiquity, *Material Research Society Proceedings* Vol 123 pp. 193-198.
- Demortier G. (1983) Topographical non destructive analysis of gold jewellery in Gold Jewelry. In: craft, style and meaning from Mycenae to Constantinopolis, T.Hackens and R.Winkes (eds), Louvain-la-Neuve, pp. 215-227.
- Demortier G. (1983) Le cadmium a-t-il été utilisé dans l'orfèvrerie antiqué? *Revue Archéologia*, n°176, pp. 41-51.
- Demortier G. (1984) Analysis of gold jewellery artefacts. *Gold Bulletin*, Vol.17, n°1, pp. 27-38.
- Demortier G. (1986) LARN experience in non-destructive analysis of gold artefacts. *Nuclear Instruments and Methods in Physics Research* B14, pp. 152-155.
- Demortier G. (1987a) *Trace analysis of medium Z elements in narrow regions of heavy matrix by XRF induced by PIXE* 11th Int.Congress on X-ray optics and micro analysis. The Univ. of Western Ontario, London (Canada) ed. pp. 147-150.
- Demortier G. (1987b) La chrysocolle des orfèvres est-elle jaune? *Archaeometry* 29(2), pp. 275-288.
- Demortier G., (1989) Ancient gold solder: what was chrysocolla? *Advances in Chemistry*, Series n°220, Archaeological Chemistry IV, R.O.Allen editor, American Chemical Society, pp. 249-263.
- Demortier G. (1991a) Etude de soudures sur quelques bijoux de l'Iran Ancien par la technique PIXE. Collection Millénaires, 2, La Découverte du métal, Picard ed., pp. 425-437.
- Demortier G. (1991b) The detection of cadmium in gold/silver alloys and its alleged occurrence in ancient gold artefacts. *Archaeometry* 33 (1991) 95-107 and *Archaeometry* 34 (112), pp. 305-310.
- Demortier G. (2021) In-vivo analysis of permanent incorporation of fluorine in tooth enamel *Dental, Oral and Maxillofacial research* 7, pp. 1-7.
- Demortier G. and Hackens T. (1982) Milliprobe and microprobe analysis of gold items of ancient jewellery, *Nuclear Instruments and Methods in Physics Research* 197, pp. 223-236.
- Demortier G., Decroupet D., Mathot S., (1987) *Brazing and soldering of gold by soft metallurgy*, Proc.11th Int.Precious Metals Inst.Conf. Brussels
- Demortier G. and Gilson A. (1987) *Determination of traces of light elements in gold artefacts using nuclear reactions*, *Nuclear Instruments and Methods in Physics Research*. B18, pp. 286-290.
- Demortier G., Decroupet D., Mathot S., (1991) Performances of PIXE and nuclear microprobes for the study of gold soldering processes, *Nuclear Instruments and Methods in Physics Research* B54, pp. 346-352.
- Demortier, G. (1992) Comment on N. D. Meeks and P. T. Craddock, 'the detection of cadmium in gold/silver alloys and its alleged occurrence in ancient gold solders' and reply comment, *Archaeometry* 34, pp. 305-312.
- Demortier G. and Morciaux Y. (1994) PIXE gadgets. *Nuclear Instruments and Methods in Physics Research* B85, pp. 112-117.
- Demortier G. and Ruvalcaba-Sil J.-L. (1996) Differential PIXE analysis of Mesoamerican Jewellery items, *Nuclear Instruments and Methods in Physics Research*. B118 (352-358)
- Demortier G., Morciaux Y., Dozot D. (1999) *PIXE, XRF and GRT for the global investigation of ancient gold artefacts*, *Nuclear Instruments and Methods in Physics Research* B 150, pp. 640-644.
- Demortier G., Quarta G., Butalak K., D'Elia M., Calcagnile L. (2008) *Benefits of combined PIXE and AMS with new accelerators*, *X-Ray Spectroscopy* 37, pp. 178-183.

- Elbern V.H. (1965) *Neue Funde Goldener Geräte des Christlichen Kultes in der Frühchristlich-Byzantinischen Sammlung*, Berlin (Akten des VII Internationalen Kongress für Christliche Archäologie – Trier).
- Flouret J., Nicolini G., Metzger C. (1981) Les bijoux d'or gallo-romains de l'Houmeau, *Gallia* 39(1), pp. 85-101.
- Guerra M.-F., Demortier G., Vitobello M.-L. Bobomulloev S., Bagault D., Borel Th., Mirasaidov I. (2009) Analytical study of the manufacturing techniques of Kushan gold jewellery (National Museum of Antiquities of Tajikistan), *ArchéoSciences* 33, pp. 177-186.
- Johansson T.B., Alselsso R., Johansson S.A.E. (1970) X-Ray Analysis: Elemental Trace Analysis at the 10⁻¹² Level. *Nuclear Instruments and Methods*, pp. 84141-143.
- Kratz A. (1972) *Goldschmiedetechnische Untersuchung von Goldarbeiten im Besitz der Skulpturenabteilung der Staatlichen Museen Preubischer Kulturbesitz Berlin* (Frühchristlich-Byzantinischen Sammlung). Sonderdruck aus Band 43 der Aachener Kunstblätter, Aachen.
- Liritzis, I., Laskaris, N., Vafiadou A., Karapanagiotis I., Volonakis, P., Papageorgopoulou, C., Bratitsi, M. (2020) Archaeometry: An overview. *SCIENTIFIC CULTURE*, Vol. 6, No. 1, pp. 49-98, DOI: 10.5281/zenodo.3625220.
- Littledale, H.A.P., (1936) U.K. Patent 415 181 .
- Meeks N.D. and Craddock PT. (1991) The detection of cadmium in gold/silver alloys and its alleged occurrence in ancient gold artefacts, *Archaeometry* 33, pp. 95-107.
- Montero I., Calligaro Th. Climent-Font A. Demortier G., Dran J.-C., Perea A. (2001) *El estudio analítico del oro in "El Tesoro Visigodo de Guarrazar"*, Libro III, Museo Arqueológico Nacional, Madrid (Spain). A.Perea ed., pp. 201-237.
- Perea, A., Gutierrez Neira, C. and Climent Font, A. (2021) Archaeometric investigation of a Hellenistic funerary belt: A case study, *Mediterranean Archaeology and Archaeometry* 18(3), pp. 1-16. DOI: 10.5281/zenodo.1461657.
- Ontalba-Salamanca M.A., Demortier G., Fernandez-Gomez F., Coquay P., Ruvalcaba-Sil J.-L. Respaldidza M.A. (1998) PIXE and SEM studies of Tartesian gold artefacts, *Nuclear Instruments and Methods in Physics Research B* 136-138, pp. 851-857.
- Quarta G., D'Elia M., Butalak K, Maruccio I., Demortier G., Calcagnile L (2006) An integrated accelerator mass spectroscopy radiocarbon dating and ion beam analysis approach for the study of archaeological contexts. *Applied Physics A* 83, pp. 605-609.
- Quarta G., D'Elia M., Butalak K, Maruccio I., Demortier G., Calcagnile L (2008) Benefits of combined PIXE and AMS with new accelerators. *X-Ray Spectroscopy* 37, pp. 178-183.
- Ruvalcaba-Sil J.-L. (1997) *Analyse non destructive par faisceaux d'ions de bijoux anciens d'Amérique*, Ph.D. thesis (University of Namur – Belgium)
- Ruvalcaba-Sil J.-L. and Demortier G. (1996) Elemental concentration profile in ancient gold artefacts by ion beam scattering. *Nuclear Instruments and Methods in Physics Research B* 113, pp. 275-278.
- Ruvalcaba-Sil J.-L., Demortier G., Oliver A. (1997) External beam PIXE analysis of gold pre-Hispanic Mexican jewelry. *International Journal of PIXE*, vol.5, n°4, pp. 273-288.
- Ruvalcaba-Sil J.-L., Guerrero G., Vargas J., Díaz E., Vázquez E. (2009) Technological and material features of the gold work of Mesoamerica. *Archeoscience* 33, pp. 289-297.
- Smit Z., Budnar M., Pelicon P., Zorko B., Knific T., Istenic J. Trampuz-Orel N., Demortier G. (2000) Analyses of gold artefacts from Slovenia, *Nuclear Instruments and Methods in Physics Research. B* 161-163, pp. 753-757.
- Solis F. and Carmona Macias M. (1993) *Mobilier funéraire des Zapothèques et Mixtèques*. Catalogue – Europalia Mexico- Kredietbank - Brussels (Belgium)
- Solis F. and Carmona Macias M (2004) *Oro Precolombino de Mexico Colecciones Mixteca y Azteca*. IXE -Landucci-Mogilner eds. Hong Kong.
- Vavpetic P., Kelemen M., Jencic B., Pelicon P. (2017) Nuclear microprobe performance in high-current proton beam mode for PIXE *Nuclear Instruments and Methods in Physics Research* 404, pp. 69-73.
- Van Oystaeyen B. and Demortier G. (1983) Matrix effects in PIXE evaluation of the major components in thick homogeneous samples, *Nuclear Instruments and Methods in Physics Research* 215, pp. 299-313.